

FIX-CLIP: Dual-Branch Hierarchical Contrastive Learning via Synthetic Captions for Better Understanding of Long Text

Bingchao Wang, Zhiwei Ning, Jianyu Ding, Xuanang Gao, Yin Li, Dongsheng Jiang, Jie Yang, Wei Liu

Shanghai Jiao Tong University, weiliucv@sjtu.edu.cn

Abstract

CLIP has shown promising performance across many short-text tasks in a zero-shot manner. However, limited by the input length of the text encoder, CLIP struggles on downstream tasks with long-text inputs (> 77 tokens). To remedy this issue, we propose FIX-CLIP which includes three novel modules: (1) A dual-branch training pipeline that aligns short and long texts with masked and raw images respectively, which boosts the long-text representation while preserving the short-text ability. (2) Multiple learnable regional prompts with unidirectional masks in Transformer layers for regional information extraction. (3) A hierarchical feature alignment module in the intermediate encoder layers to promote the consistency of multi-scale features. Furthermore, we collect 30M images and utilize existing MLLMs to synthesize long-text captions for training. Extensive experiments show that FIX-CLIP achieves state-of-the-art performance on both long-text and short-text retrieval benchmarks. For downstream applications, we reveal that FIX-CLIP’s text encoder delivers promising performance in a plug-and-play manner for diffusion models with long-text input.

1. Introduction

CLIP [39] has garnered significant performance across various open-vocabulary tasks. It is widely used as the backbone in Multi-modality Large Language Model (MLLM) [3, 26, 27, 50] and generative models like Stable Diffusion [41].

The success of CLIP is based on the large-scale web-based image-text pairs, which have extremely short effective text length [57]. In fact, images often require dozens of sentences to describe their content adequately. However, CLIP can not understand long text inputs, which severely limits its application to MLLMs and text-to-image generation models. Recently, PixArt- α [4] uses Flan-T5 as the text encoder to increase the length of input tokens from 77 to 120 and injects the obtained text features into DiT [37] to alleviate the deficiency in long-text understanding. Following Long-CLIP [57], our model achieves stronger performance with

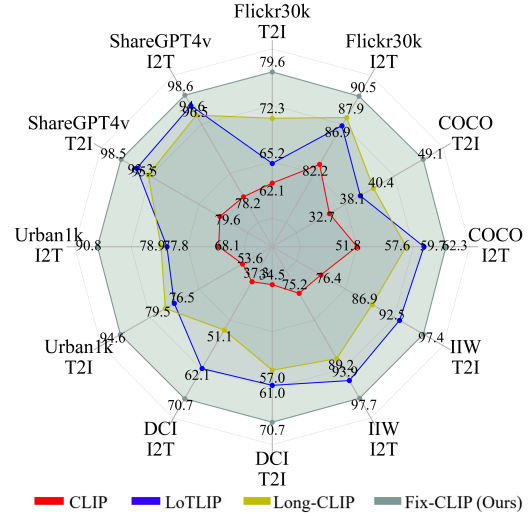


Figure 1. We compare FIX-CLIP with CLIP [39], LoTLIP [51], and Long-CLIP [57] on B/16 model. FIX-CLIP achieves competitive performance across long-text and short-text retrieval tasks.

an input length of 248.

To improve the understanding of long text, previous methods [51, 57, 60] incorporate long caption datasets to enhance the alignment between image and long-text while maintaining the short-text performance through pre-training [51, 60] or incremental training [57] strategy. Nonetheless, the conventional training paradigm of contrastive learning aims to convert the [CLS] tokens of images and texts into a consistent feature space, which emphasizes global alignment rather than local alignment. The lack of local representation and long-text understanding leads to suboptimal performance on tasks requiring fine-grained description.

Due to the reason that effective extraction of image detail features is crucial, recent works [1, 43, 49] make an effort to address the issue by dividing the input images into several regions and matching each region with the corresponding caption. These methods facilitate the detailed representation of image features explicitly. Furthermore, some methods [24, 30, 34] match patch embeddings in the image encoder middle layers with text features to imple-



Figure 2. Comparison of FIX-CLIP against Long-CLIP [57] in image-to-text and text-to-image retrieval tasks with long-text captions. The key texts related to the correct elements are marked in green, and the red texts indicate the wrong elements.

itly enhance regional consistency. The explicit approaches need to generate corresponding captions for numerous image regions, leading to large data scales and high resource occupation. Conversely, methods that focus on implicit local consistency [24, 30] would inadvertently impact the generalization capability of the pre-trained model, resulting in the degraded performance of short-text tasks.

In this work, we optimize the implicit alignment strategy and conduct incremental training on the pre-trained model to achieve a balance between performance and resource consumption. We propose FIX-CLIP to improve the understanding of long text and maintain the superior generalization ability in short-text tasks, as shown in Fig. 1. Fig. 2 visualizes our superiority over vanilla CLIP [39] and Long-CLIP [57] in image-text retrieval tasks. The contributions of this paper are as follows:

- A dual-branch training pipeline is proposed to align short and long texts with masked and raw images respectively. It enhances long-text capabilities while preventing the forgetting of CLIP’s original short-text abilities.
- Regional prompts are designed for better alignment between sub-texts and local visual features, assisted with a unidirectional mask to preserve the integrity of the patch embedding.
- A hierarchical feature alignment module is employed to promote the consistency of multi-scale features in the intermediate encoder layers, which optimizes contrastive learning in long texts.
- We instruct MLLMs to synthesize 30M long-text-image pairs for training. Our FIX-CLIP achieves state-of-the-art performance on long-text and short-text benchmarks. The text encoder delivers promising performance in a plug-and-play manner for diffusion models with long-text input.

2. Related Work

2.1. Vision-Language Pre-training Model

CLIP serial approaches [8, 20, 39, 53, 58] effectively mitigate the inconsistency in feature spaces between the output of the text encoder and the image encoder by restricted alignment strategy. As the pioneering works, CLIP [39] and

ALIGN [20] demonstrate that leveraging internet-sourced dataset (400M) enables promising results across computer vision tasks, including classification [43, 45], segmentation [11, 19, 25, 59, 61] and detection [14, 28, 44]. The similar image and text encoder are designed to extract multi-modal information and project them into a shared space to achieve feature alignment.

Benefiting from the generalization ability of CLIP, many subsequent methods [11, 29, 45, 46, 54] achieve promising performance in open-world scenes. MaskCLIP [11] and FLIP [29] enhance the encoding capability by masking a large proportion of image patches. FILIP [54] explores regional expressiveness by facilitating the consistency between patch tokens and text tokens. EVA-CLIP [45] conducts novel techniques for stable and efficient training. However, the capability of long-text understanding remains the limitation of CLIP [39], which restricts the development of more complex vision-language applications.

2.2. Long Text Understanding

For computational efficiency, the sequence length is capped at 77 in CLIP, which prevents the subsequent information in long text. An image usually contains rich information and requires a lengthy caption to be described. In recent works, instructing LLMs or MLLMs to synthesize data has become a cost-effective choice for data synthesis. LaCLIP [12] directly rewrites the original text descriptions through LLMs, which leads to serious hallucinations. VeCLIP [23] and CAPSFUSION [55] inject visual concepts extracted from images into captions with the help of MLLMs, enriching the text content. SynthCLIP [15] uses text-to-image models to synthesize images and explores fully synthetic CLIP training.

Several works [51, 57, 60] focus on releasing the potential of the long text understanding. Long-CLIP [57] reveals that the effective length for CLIP is merely 20 tokens, and fine-tunes the CLIP model by the long captions from ShareGPT4V [6], but it leads to a decline on short text tasks. TULIP [35] replaces absolute positional encodings with rotary positional encodings (RoPE) and initializes a new text encoder using model distillation. But the degrada-

tion of short-text abilities is severe, recent works (DreamLIP [60], LoTLIP [51], and FLAIR [52]) have to train from scratch on synthetic datasets generated by InstructBLIP [9], LLaVA [31] and ShareGPT4V [6]. But these works only use a simple prompt “Describe the image in detail” to synthesize captions on CC3M [42], CC12M [42] and YFCC15M [47].

3. Method

FIX-CLIP utilizes the incremental training in the synthetic dataset and consists of three components as illustrated in Fig. 3. The process of long captions synthesis and cleaning is introduced in Sec. 3.1. In Sec. 3.2, we introduce a dual-branch training pipeline. In Sec. 3.3, the regional prompts with unidirectional mask are proposed to extract regional features for fine-grained description. The hierarchical features alignment module proposed in Sec. 3.4 aligns the intermediate features in the image encoder and text encoder for contrastive learning.

3.1. Long-Text Dataset Synthesis and Cleaning

We adopt Llama3-LLaVA-NeXT-8b [32] to synthesize detailed descriptive long captions. To ensure diversity, we set 20 diverse prompts for synthesis, which are listed in Appendix 6. The average length of the synthetic captions is around 120 tokens, which is longer than 18 tokens in the raw captions. We also use Shikra [5] to synthesize short captions for exploration. We demonstrate the superiority of synthesized short captions over original short captions in Tab. 10 and Tab. 11 of the Appendix.

We construct three different scales of synthetic data: (1) **5M**, including CC3M [42], VisualGenome [21], ShareGPT4V [6] and SBU [36]. (2) **15M**, including **5M** and CC12M [42]. (3) **30M**, including **15M** and YFCC15M [47]. Because MLLMs usually bring hallucination information, we removed low-quality captions including repeated words, meaningless sentences, and short results. Some low-quality examples are shown in Appendix 7. The final training data details are shown in Tab. 8 of the Appendix.

3.2. Dual-Branch Training Pipeline

It is essential to design distinct encoding strategies for texts of varying lengths to enhance the expressiveness of long texts while maintaining the feature extraction capabilities for short texts. To achieve this, we retain the parameters of the text Transformer blocks from the pre-trained model and modify the position embeddings. In detail, we inherit all the 77 raw position embeddings PE from the pre-trained model and freeze the parameters for short texts. For long texts, we freeze the first 20 position embeddings because the preceding tokens can summarize the major description of the total texts [57]. Then, we expand the remaining position embeddings (from 21 to 77) through the interpolation method

to reach four times of the original length, denoted as:

$$\begin{aligned} PE_l &= \text{Concat}(PE[:20], \text{Intpol}(PE[20:], 4)), \\ \text{Intpol}(PE, q)[i] &= (1 - \lambda) * PE[\lfloor \frac{i}{q} \rfloor] + \\ &\quad \lambda * PE[\lfloor \frac{i}{q} \rfloor + 1], \quad \lambda = \frac{i \% q}{q}, \end{aligned} \quad (1)$$

where $\lfloor \cdot \rfloor$ defines the floor function. q and i denote the index of the interpolated ratio and the interpolation position, while λ represents the assigned weight.

Consequently, the length of the position embeddings for long texts PE_l increases to 248, adequately meeting the requirements in most scenarios. During the training, the parameters of these expanded embeddings are updated to facilitate the extraction of the postpositional information in the text.

Texts of diverse lengths usually correspond to distinct feature spaces, which require customized image features to match. MAE [17] claims that 75% random masked image retains sufficient semantic information. Therefore, aligning random masked images with short captions is an efficient and low-cost pipeline. Specifically, given the raw image patch embeddings $I \in \mathbb{R}^{N \times D}$, we randomly replace $\alpha \times N$ patch embeddings with learnable parameters initialized by 0 to denote the masked images I_m , where α is the mask ratio and is set as 0.75 at first. Then, we consider the masked image patches I_m and short texts T_s as the pairs for contrastive learning. Conversely, the long texts often include specific details retained in the raw images. Therefore, we take the raw image patches I and long texts T_l as input pairs.

3.3. Regional Prompts with Unidirectional Mask

The [CLS] token interacts with all patch embeddings via the attention mechanism to aggregate the global visual features in the image encoder. However, the capability to recognize local information is insufficient. To address this issue, we introduce several learnable parameters as regional prompts and leverage an unidirectional attention mask to ensure that these prompts attend only to the corresponding regions in the image. Specifically, in the l -th Transformer block layer of the image encoder, we interpolate the initial input sequence $([CLS], P_1, \dots, P_N)$ with M learnable prompts to define our input $([CLS], R_1^l, \dots, R_M^l, P_1, \dots, P_N)$, where $P_i (i \in [1, N])$ represents the i -th patch embedding and $R_j^l (j \in [1, M])$ denotes the j -th regional prompt. After the Multi-Head Self-Attention (MHSA) in the l -th layer, the input sequences are encoded to $\mathbf{X}^l \in \mathbb{R}^{(1+M+N) \times D}$ where D is the dimension of the channel. Subsequently, each regional prompt R_j^l in \mathbf{X}^l is replaced with a new learnable regional prompt from the next layer R_j^{l+1} :

$$\mathbf{X}^l[1 : 1 + M] = (R_1^{l+1}, \dots, R_M^{l+1}). \quad (2)$$

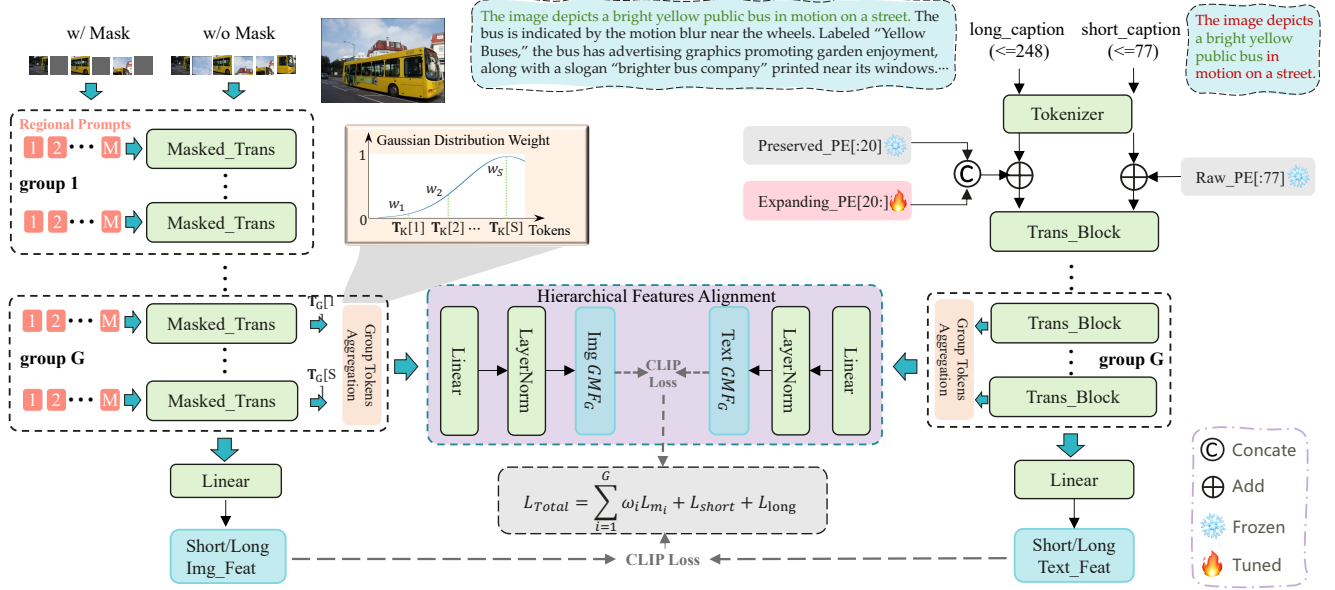


Figure 3. Overview of FIX-CLIP. The image w/o mask aligns with a long caption, while the masked image aligns with a short caption. In the image encoder, regional prompts are employed with the unidirectional mask to extract the regional information. The hierarchical alignment module is designed to associate the middle aggregation features between the image encoder and the text encoder.

The procedure above enables each prompt to focus solely on the local features in the current layer, which eliminates the interference of information across different depth layers.

During multi-head self-attention, we additionally implement an unidirectional attention mask **Mask** to allow the regional prompts to concentrate on the specific local patches while preserving the integrity of the original patch embeddings. As illustrated in Fig. 4, each row represents the mask vector of a query Q , which is implemented as follows: the [CLS] token attends to itself as well as all the regional prompts and patch embeddings; the patch embedding P_i focuses on the non-regional prompts partition; each regional prompt R_j attends only to itself and the patch embeddings in the related region, whose mask vector is defined as:

$$\text{Mask}[R_j] = \mathbb{1}(j, b_j, \dots, b_j + \lfloor \frac{N}{M} \rfloor - 1), \quad (3)$$

$$b_j = 1 + M + j \times \lfloor \frac{N}{M} \rfloor,$$

where $\mathbb{1}(\cdot) \in \mathbb{R}^{1+M+N}$ presents the flag function that the indicated positions are set as 1 while other places are defined as 0, and $\lfloor \cdot \rfloor$ is the floor function. b_j denotes the first index of the patches corresponding to the current prompt R_j . This method effectively promotes the extraction of local information within regional prompts while restraining the influence of patch embeddings. Then, we multiply the proposed **Mask** with the mask map calculated from the self-attention in an element-wise manner to obtain our final attention mask. The $(l+1)$ -th Transformer block encoder

$\mathcal{T}_{\text{MHSA}}^{l+1}(\cdot)$ can be formulated as follows:

$$\begin{aligned} \mathbf{X}^{l+1} &= \mathcal{T}_{\text{MHSA}}^{l+1}(\mathbf{X}^l) \\ &= \text{softmax}\left(\frac{QK^T}{\sqrt{d}} \odot \text{Mask}\right)V, \end{aligned} \quad (4)$$

where \mathbf{X}^l and \mathbf{X}^{l+1} are the input and the output of $\mathcal{T}_{\text{MHSA}}^{l+1}(\cdot)$. Q , K and V are calculated by multiplying \mathbf{X}^l with the learnable weights W_Q , W_K and W_V , and d is the channel number of Q and K .

3.4. Hierarchical Feature Alignment

Because of the superior complexity of the long text feature spaces, it is not enough to build only the correlation on the vision-language features of the last layer. The intermediate layer features should also exhibit consistency, and this can be achieved via a hierarchical feature alignment module. To be specific, given that there are total L Transformer block layers in the image encoder, $T_l = \mathbf{X}^l[0]$ denotes the [CLS] token in the l -th layer. Then, all the L tokens are divided into G groups uniformly with each group containing $S = L/G$ tokens, and the g -th group is denoted as \mathbf{T}_g . Then, the Gaussian distribution weights are utilized for Group Tokens Aggregation (GTA) as follows:

$$\text{GTA}(\mathbf{T}_g) = \sum_{j=1}^S \text{Gaussian}(j; S, 1) * \mathbf{T}_g[j]. \quad (5)$$

Subsequently, the aggregated features $\text{GTA}(\mathbf{T}_g)$ will be fed into a linear projection layer, followed by a layer

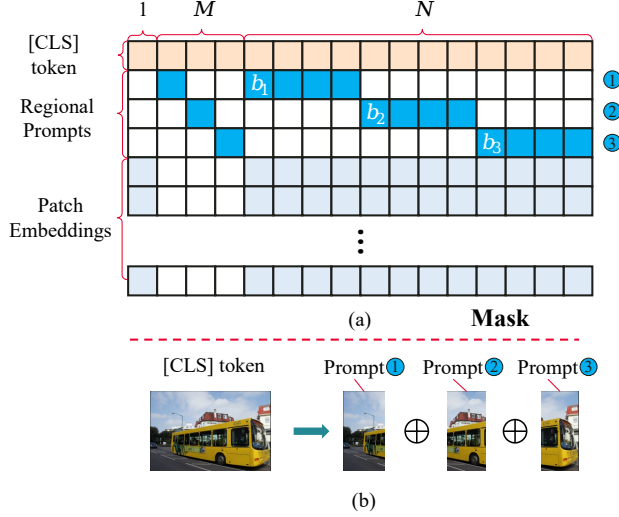


Figure 4. Unidirectional mask map is proposed to achieve the unidirectional information propagation from patches to prompts. (a) The illustration of **Mask** map. (b) The [CLS] token attends to the global description but each prompt enables to focus on a specific region.

normalization operator to calculate the g -th Group Middle Feature (GMF):

$$GMF_g = LN(Proj(GTA(\mathbf{T}_g))). \quad (6)$$

As for the text branch, all of the Transformer blocks are also divided into G groups, followed by the similar strategy above to obtain GMF for the long caption. We also empirically observe that the image features and text features in the shallow layers exhibit larger divergence compared to those in the deeper layers, as shown in Sec. 4.4. Therefore, we only align the GMF from the K -th to the G -th group to reduce the computational cost and accelerate model convergence. Furthermore, we utilize the Information Noise Contrastive Estimation (InfoNCE) [16] to calculate the loss L_{m_i} of GMF:

$$L_{m_i} = - \sum_{j=1}^B \log \frac{\exp(\cos\langle v_i^j, t_i^j \rangle / \tau)}{\sum_{k=1}^B \exp(\cos\langle v_i^j, t_i^k \rangle / \tau)} - \sum_{j=1}^B \log \frac{\exp(\cos\langle t_i^j, v_i^j \rangle / \tau)}{\sum_{k=1}^B \exp(\cos\langle t_i^j, v_i^k \rangle / \tau)}, \quad (7)$$

where B denotes the batch size, v_i and t_i represent the GMF of the image and text in the i -th group. Finally, we multiply each L_{m_i} with weight ω_i and sum up them with the InfoNCE loss of short-text-image pairs L_{short} and long-text-image pairs L_{long} . The final contrastive loss for model training is formulated as:

$$L = \sum_{i=K}^G \omega_i L_{m_i} + L_{short} + L_{long}. \quad (8)$$

4. Experiments

4.1. Experimental Setup

Downstream datasets. To evaluate the effectiveness of our model, we select three zero-shot tasks following [57]: short-text-image retrieval, long-text-image retrieval, and image classification. For long-text-image retrieval, following LoTLIP [51] and Long-CLIP [57], we evaluate method on datasets with long captions, including ShareGPT4V-1k [6], Urban-1k [57], DCI [48], and IIW [13] and report the Recall at 1 (R@1) metric. In DCI [48] and IIW [13], all images with human-authored long captions are used for evaluation. For short-text-image retrieval, we use the 5k validation set of COCO [7] and 1k test set of Flickr30k [38] for evaluation and present the Recall at 1, 5 and 10 (R@1, R@5 and R@10). For image classification, we evaluate on ImageNet-1K [10], ImageNet-V2 [40], ImageNet-O [18], ImageNet-A [18], CIFAR-10 [22] and CIFAR-100 [22] and report the top-1 Accuracy (Acc@1).

Training setup. For a fair comparison, our experiment setup follows Long-CLIP [57]. For results without specifically indicating data scales, the training dataset is ShareGPT4V [6], which contains 1M long-text-image pairs. For results with data scales, the training datasets are our synthetic data. Two variants of Vision Transformer are used as the image encoder in our experiments, *i.e.* ViT-B/16 and ViT-L/14, while the text encoder is a vanilla Transformer. The image size is 224×224 , and the input text sequence length is truncated or padded to 248. We train the model on $16 \times$ A800 GPUs with a batch size of 2048. The other hyperparameters are under the same setting as Long-CLIP [57] (*e.g.*, learning rate, warmup steps, and weight decay). Detailed training settings are shown in Appendix 8.

4.2. Comparison with Previous Methods

In this section, our method is trained on ShareGPT4V [6] (1M) and tested on numerous open-vocabulary benchmarks, including zero-shot retrieval and classification. We compare FIX-CLIP against the state-of-the-art approaches to prove the effectiveness of our method.

Long text-image retrieval. The results in Tab. 1 demonstrate that FIX-CLIP has superior ability in long-text understanding. Comparing models trained on ShareGPT4V(1M), FIX-CLIP surpasses Long-CLIP in the long text-image retrieval task, obtaining higher R@1 scores on both DCI (I2T: +8.6%, T2I: +6%) and IIW (I2T: +4.6%, T2I: +8.7%) datasets. The average improvements with ViT-B/16 and ViT-L/14 image encoders can even achieve 5.8% and 7.3% compared to Long-CLIP.

Short text-image retrieval. Tab. 2 shows the main results of short-text-image retrieval in COCO [7] and Flickr30k [38] datasets. With the B/16 encoder, FIX-CLIP outperforms Long-CLIP [57] in the text-to-image retrieval task, obtain-

	Method	Data	DCI		IIW		ShareGPT4V-1k		Urban-1k		Avg.
			I-to-T	T-to-I	I-to-T	T-to-I	I-to-T	T-to-I	I-to-T	T-to-I	
B/16	CLIP* [39]	400M	37.3	34.5	75.2	76.4	78.2	79.6	68.1	53.6	62.8
	Fine-tuned CLIP	1M	46.3	45.4	87.4	85.6	94.1	93.6	80.4	79.8	76.6
	Long-CLIP [57]	1M	51.1	57.0	89.2	86.9	94.6	93.3	78.9	79.5	76.8
	FIX-CLIP	1M	59.7	63.0	93.8	95.6	95.5	94.1	80.9	81.1	82.6
	SigLIP* [56]	12B	57.8	56.2	91.9	91.0	85.8	83.4	62.7	62.1	73.9
	FLAIR* [52]	30M	61.3	66.2	-	-	98.5	98.0	83.6	87.7	-
	LoTLIP* [51]	100M	62.1	61.0	93.9	92.5	96.5	95.5	77.8	76.5	81.9
	Fix-CLIP	5M	67.1	67.5	96.9	96.7	98.1	97.9	88.0	90.8	87.8
	Fix-CLIP	15M	69.2	69.9	97.1	97.2	98.3	98.2	88.0	93.7	88.9
	Fix-CLIP	30M	70.7	70.7	97.4	97.4	98.6	98.5	90.8	94.6	89.8
L/14	CLIP* [39]	400M	37.9	35.9	78.6	80.2	81.8	84.0	68.7	52.8	65.0
	Fine-tuned CLIP	1M	46.9	46.2	88.6	88.5	95.3	95.4	78.0	76.5	76.9
	Long-CLIP [57]	1M	51.7	57.4	91.2	90.1	95.8	95.6	82.7	86.1	79.2
	FIX-CLIP	1M	65.1	66.7	96.2	97.1	98.1	98.6	86.8	87.7	85.8
	Fix-CLIP	5M	68.1	69.9	97.1	97.2	98.5	98.0	88.1	93.0	88.7
	Fix-CLIP	15M	69.2	70.2	97.7	98.1	98.7	98.1	89.5	94.3	89.5
	Fix-CLIP	30M	72.0	74.2	97.9	98.2	99.0	98.3	93.7	96.3	91.2

Table 1. Zero-shot long text-image retrieval benchmarks. I2T and T2I indicate the R@1 score on image-to-text and text-to-image retrieval. SigLIP [56], LoTLIP [51] and FLAIR(30M) [52] do not have L/14 results. *models are trained from scratch. The best results are **bold**.

ing higher R@1 scores on COCO (+4.4%), and Flickr30k (T2I: +5.1%) datasets. FIX-CLIP surpasses Long-CLIP with an average 2.2% improvement with the ViT-L/14 image encoder in the R@1 metric. FIX-CLIP also outperforms TULIP [35] which uses two-stage training with distillation and fine-tuning on 1M data. The above results show that FIX-CLIP can enhance the long-text understanding while maintaining the generalization capability on short-text tasks. **Zero-shot classification tasks.** As shown in Tab. 3, FIX-CLIP also achieves promising performance. In particular, FIX-CLIP attains a remarkable improvement on two challenging adversarial out-of-distribution datasets, ImageNet-O [18] and ImageNet-A [18]. FIX-CLIP provides robustness and generalization capabilities of FIX-CLIP in handling complex and adversarial scenarios.

4.3. Scalability Analysis

Due to the degradation of short-text capabilities, recent works have to train from scratch on reconstructed datasets, incurring high resource costs. Our method employs incremental training and aligns with CLIP’s original short-text feature space better.

We further inspect the scalability of FIX-CLIP across three data scales: 5M, 15M, and 30M. Our investigation in Tab. 1 reveals that synthetic long-text captions exhibit remarkable scalability. When including SOTA models, FIX-CLIP trained on 5M synthetic data and B/16 image encoder outperforms SigLIP, FLAIR, and LoTLIP on all pre-training datasets by a large margin. When we move to larger datasets with 30M synthetic data, FIX-CLIP surpasses the previous SOTA in the long text-image retrieval task, obtaining higher R@1 scores on DCI (I2T: +8.6%, T2I: +9.7%), IIW (I2T:

+3.5%, T2I: +4.9%), and Urban-1k (I2T: +7.2%, T2I: +6.9%) datasets.

Models like EVA-CLIP and FLIP are pre-trained on large short-text datasets, with EVA-CLIP even trained at a 2 billion scale. This leads to significant degradation of short-text capabilities in prior long-text understanding works. Benefiting from our training pipeline, CLIP’s original short-text abilities are preserved and continuously enhanced with increased training data. As shown in Tab. 2, with 30M training data, FIX-CLIP outperforms the previous work in the text-to-image retrieval task, obtaining higher R@1 scores on COCO (+6.9%), and Flickr30k (T2I: +8.4%) datasets.

In summary, FIX-CLIP outperforms state-of-the-art approaches by 13% and 5% on long-text and short-text benchmarks, respectively.

4.4. Ablation Study

Model Components. To assess the effectiveness of the proposed modules, we conduct the ablation studies through incremental training on the ShareGPT4V [6] dataset. The image encoder is ViT-L/14 [2] and the text encoder is the same as [39]. In Tab. 4, we analyze the components of FIX-CLIP: dual-branch training pipeline (DB), hierarchical feature (HF) alignment, regional prompts (RP), and unidirectional mask (UM).

Long-CLIP [57] is the baseline of the ablation (0). Changing the training pipeline to the dual-branch (DB) type leads to performance improvements across all metrics (1), achieving an 8.8%/4% boost in R1 for DCI long text-image retrieval, which demonstrates its contribution to long-text understanding. Hierarchical feature (HF) alignment also provides decent gain for all benchmarks (2). Adding regional

		COCO							Flickr30k							Avg.
Method	Data	Image-to-Text			Text-to-Image			Image-to-Text			Text-to-Image			R@1		
		R@1	R@5	R@10	R@1	R@5	R@10	R@1	R@5	R@10	R@1	R@5	R@10			
B/16	CLIP* [39]	400M	51.8	76.8	84.3	32.7	57.7	68.2	82.2	96.6	98.8	62.1	85.7	91.8	57.2	
	Long-CLIP [57]	1M	57.6	81.1	87.8	40.4	65.8	75.2	87.9	97.2	98.9	72.3	92.2	95.6	64.6	
	TULIP [35]	1M	56.8	80.3	-	40.7	66.1	-	86.9	96.4	-	73.7	93.6	-	64.5	
	Fix-CLIP	1M	60.9	83.4	90.2	44.8	70.2	79.5	88.4	98.5	99.5	77.4	94.8	97.1	67.9	
	EVA-CLIP* [45]	2B	58.7	80.7	88.2	42.2	66.9	76.3	85.7	96.7	98.9	71.2	91.0	94.7	64.5	
	LoTLIP* [51]	30M	59.7	81.5	-	38.1	63.8	-	86.9	97.8	-	65.2	88.0	-	62.5	
	DreamLIP* [60]	30M	58.3	81.6	88.8	41.1	67.0	76.6	87.2	97.5	98.8	66.4	88.3	93.3	63.3	
	Fix-CLIP	5M	61.3	84.9	91.2	47.0	72.4	81.4	89.9	98.8	99.7	78.4	95.2	97.7	69.2	
	Fix-CLIP	15M	61.2	84.7	91.8	48.7	74.3	82.7	89.1	98.4	99.7	79.5	95.1	97.6	69.6	
	Fix-CLIP	30M	62.3	85.4	91.4	49.1	73.8	82.4	90.5	99.0	99.8	79.6	94.9	97.4	70.4	
L/14	CLIP* [39]	400M	56.3	79.3	86.7	36.5	61.0	71.1	85.2	97.3	99.0	65.2	87.3	92.0	60.8	
	Long-CLIP [57]	1M	58.3	81.4	88.2	45.1	70.4	79.3	90.9	98.8	99.5	78.7	94.5	97.1	68.3	
	TULIP [35]	1M	62.6	84.7	-	46.1	71.1	-	92.3	99.3	-	79.0	94.8	-	70.0	
	Fix-CLIP	1M	63.4	85.8	91.4	46.5	72.0	80.7	93.0	99.5	99.6	79.2	95.9	97.4	70.5	
	FLIP* [29]	400M	60.2	82.6	89.9	44.2	69.2	78.4	89.1	98.5	99.6	75.4	92.5	95.9	67.2	
	EVA-CLIP* [45]	2B	63.7	84.3	90.4	47.5	71.2	79.7	89.7	98.6	99.2	77.3	93.6	96.8	69.6	
	Fix-CLIP	5M	63.2	85.8	91.5	50.5	75.4	83.6	92.5	99.1	99.9	82.5	96.6	98.2	72.1	
	Fix-CLIP	15M	63.7	86.8	92.1	51.9	76.2	84.4	90.7	99.3	99.9	83.8	96.6	98.3	72.5	
	Fix-CLIP	30M	64.5	86.5	91.9	52.6	77.2	84.9	91.5	99.8	99.9	84.1	96.7	98.4	73.2	

Table 2. Results of zero-shot short text-image retrieval on the COCO [7] validation set and the 1k Flickr30K [38] test set. LoTLIP [51] and DreamLIP [60] do not provide L/14 results. FLIP [29] does not provide B/16 results. *models are trained from scratch. The best results are **bold**.

Method	IN-1k	IN-O	IN-A	IN-V2	Cifar10	Cifar100	Average
B/16	CLIP [39]	68.4	42.2	38.4	61.9	90.8	67.3
	Fine-tuned CLIP	55.1	31.7	30.5	44.8	83.9	59.2
	Long-CLIP [57]	66.8	<u>42.7</u>	<u>46.0</u>	61.2	90.7	<u>69.3</u>
	Fix-CLIP	<u>68.0</u>	44.1	49.8	<u>61.8</u>	91.9	70.6
							64.4
L/14	CLIP [39]	75.5	31.9	46.4	69.9	<u>95.5</u>	76.8
	Fine-tuned CLIP	58.4	29.2	35.8	52.7	92.7	68.7
	Long-CLIP [57]	73.5	<u>33.7</u>	<u>61.0</u>	67.9	95.3	<u>78.5</u>
	Fix-CLIP	<u>73.7</u>	35.9	66.7	<u>68.8</u>	96.2	78.9
							71.4

Table 3. Top-1 accuracy for zero-shot classification on: ImageNet-1K [10], ImageNet-O [18], ImageNet-A [18], ImageNet-V2 [40], CIFAR-10 [22] and CIFAR-100 [22]. The best and second-best results are **bold** and underlined.

prompts (RP) improves the performance in each task (3 and 4). The interpolation of regional prompts (RP) further improves the performance of Fix-CLIP in various metrics and even achieves the best performance on COCO’s T2I task (5 and 6). Additionally, the unidirectional mask (UM) alleviates the degradation of generalization capability in short texts, achieving 0.9% improvement in image-to-text retrieval on the COCO [7] dataset. Fix-CLIP with all components achieves the best performance (7). Overall, the dual-branch training pipeline is the foundation of Fix-CLIP, giving the ability to understand long text, while other components contribute to continued performance growth.

Ablation on different input schemes. In the default implementation, the same position embedding is used for short and long texts, and only the original image patches are utilized

	Method				DCI		IIW		COCO	
	DB	HF	RP	UM	I2T	T2I	I2T	T2I	I2T	T2I
0					51.7	67.4	91.2	90.1	58.3	45.1
1	✓				60.5	61.4	94.0	95.2	60.9	45.9
2		✓			53.3	58.5	91.9	92.3	59.6	45.3
3	✓		✓		62.4	62.6	94.5	95.6	61.7	46.1
4		✓	✓		54.5	59.8	92.8	92.7	60.3	45.6
5	✓		✓	✓	63.5	63.1	95.9	96.1	63.0	46.8
6		✓	✓	✓	56.3	62.7	93.5	93.7	61.2	45.9
7	✓	✓	✓	✓	65.1	66.7	96.2	97.1	63.4	46.5

Table 4. Ablation study on different components of Fix-CLIP. **DB**: Dual-Branch training pipeline, **HF**: Hierarchical Feature alignment, **RP**: Regional Prompts, **UM**: Unidirectional Mask.

for feature extraction. When we modify the position embedding strategies to accommodate texts of varying lengths, the improvement can be observed in the retrieval task, as shown at the top of Tab. 5. Furthermore, aligning the masked image features with short caption features results in higher recall. We also find that preserving the original length of image patches by replacing the masked patch embeddings with learnable parameters yields better performance. As shown at the bottom of Tab. 5, although discarding the masked patches reduces the computational cost and memory occupancy, the recall significantly drops compared to the strategy that preserves the length.

Ablation on the number of regional prompts. The ablation study in Tab. 6 investigates the optimal number of regional prompts, which is represented by M in Sec. 3.3. We interpolate different numbers of prompts in the image encoder.

Init.	Pos.	Pre.	Dis.	DCI		COCO		Mem./G	Time/ms
				I2T	T2I	I2T	T2I		
✓	✗	✗	✗	62.6	62.9	61.2	45.9	–	–
✗	✓	✗	✗	64.3	64.2	62.1	46.1	–	–
✗	✓	✓	✗	65.1	66.7	63.4	46.5	17.2	61.92
✗	✓	✗	✓	62.7	63.4	62.0	45.3	16.3	58.32

Table 5. Ablation on different inputs schemes. “Init.” means the configuration of position embedding follows Long-CLIP [57]. “Pos.” means conducting the different position embedding for texts. “Pre.” means preserving the masked image patches, and “Dis.” means discarding the masked image patches. “Mem./G” and “Time/ms” are memory occupancy and time cost on a A800 GPU.

UM	Num.	DCI		COCO	
		I2T	T2I	I2T	T2I
✗	0	60.9	62.7	62.7	46.4
✗	4	62.5	64.0	62.9	46.2
✓	1	62.7	64.3	63.6	46.3
✓	2	64.2	64.5	63.1	46.4
✓	4	65.1	66.7	63.4	46.5
✓	8	64.8	65.4	63.0	46.5

Table 6. Ablation on the number M of regional prompts. “UM” means utilizing the unidirectional mask. “Num.” means the number of regional prompts.

A larger number of regional prompts allows each prompt to attend to a smaller region, enabling finer-grained information capture, as described in Eq. (3). Interestingly, when the number of regional prompts is 1, the image-text retrieval performance on COCO is the highest, demonstrating that more regional prompts aid in extracting local features, while fewer prompts benefit short-text image-text retrieval. When the number of prompts is set to 4, our approach achieves the best performance on average.

Ablation on different groups of hierarchical feature alignment. As a more reasonable contrastive learning strategy, hierarchical alignment also demonstrates its effectiveness in long-text tasks. We divide all the Transformer blocks into 6 groups both in the image encoder and the text encoder. As illustrated in Tab. 7, applying the hierarchical contrastive learning from the 4-th group to the 6-th group achieves 1.6%/3.6% improvement on the DCI benchmark. The last column shows that the GMF loss steadily decreases as the group depth increases. Moreover, the weight of each GMF loss should increase incrementally, as deeper features are more critical for alignment. Finally, we set the weights for GMF loss as 0.2, 0.4, and 0.8 for 4-th, 5-th, and 6-th groups, respectively.

Other Ablations. It should be noted that we employ long position embeddings across all downstream tasks when referring. The performance comparison of different position embeddings is shown in Tab. 13 of the Appendix. Tab. 13 also presents more ablations on the efficacy of region prompts and masks.

Hier	Groups	DCI		COCO		GMF Loss Avg.
		I2T	T2I	I2T	T2I	
w/o	–	63.5	63.1	63.1	46.5	–
w/	[1, 6]	64.0	63.9	63.1	46.3	4.48
w/	[3, 6]	64.8	65.4	62.8	46.1	3.49
w/	[4, 6]	65.1	66.7	63.4	46.5	2.65
w/	[5, 6]	64.7	65.6	62.7	46.2	1.71

Table 7. Ablation on the hierarchical contrastive learning with different groups included.

A shiny, grey-blue Morris Minor Traveller car is parked facing left on a black cobblestone street in dappled sunlight in an eye-level outdoor shot. The car has large front fenders that extend into the doors, and large rear fenders bordered in light-brown wood. The front of the car has a cabin space for two people, while the back end of the car has a flat white roof, a border of light-brown wood, and cargo space for objects. The tires are black, but the sidewalls are white, while the hubcaps are shiny chrome with red centers.



Long-CLIP

Fix-CLIP (Ours)

Figure 5. Comparison on the text-to-image generation performance. We replace the text encoder in the stable diffusion model with our or Long-CLIP’s text encoder.

4.5. Text-to-Image Generation

FIX-CLIP can be integrated into Stable-Diffusion-XL for text-to-image generation in a plug-and-play manner. We replace the CLIP-L text encoder with FIX-CLIP-L. Benefiting from the effective modules, FIX-CLIP outperforms Long-CLIP [57] in understanding long texts. As demonstrated in Fig. 5, images generated by FIX-CLIP better represent detailed information in long texts, such as object orientation, material, color, background, and interaction details. More generated images are provided in Appendix 9.

5. Conclusion

In this work, we propose FIX-CLIP to improve the long-text understanding capability while preserving the short-text ability of CLIP. Considering the distinct feature spaces between short and long texts, we design a dual-branch training pipeline to align short and long texts with masked and raw images respectively. Then, the learnable regional prompts with unidirectional masks are proposed to extract the local features from patch embeddings. We employ a hierarchical alignment module to establish more precise correspondence between intermediate-level textual and visual representations. To explore the performance limits of our model, we leverage MLLMs to synthesize long captions from 30M images and clean the data for training. FIX-CLIP outperforms prior works on numerous open-vocabulary tasks across various training data scales and serves as an effective backbone for diffusion models.

References

- [1] Ali Abdollah, Amirmohammad Izadi, Armin Saghafian, Reza Vahidimajd, Mohammad Mozafari, Amirreza Mirzaei, Mohammadmahdi Samiei, and Mahdieh Soleymani Baghshah. Comalign: Compositional alignment in vision-language models. *arXiv preprint arXiv:2409.08206*, 2024. 1
- [2] Dosovitskiy Alexey. An image is worth 16x16 words: Transformers for image recognition at scale. *arXiv preprint arXiv:2010.11929*, 2020. 6
- [3] Zheng Cai, Maosong Cao, Haojiong Chen, Kai Chen, Keyu Chen, Xin Chen, Xun Chen, Zehui Chen, Zhi Chen, Pei Chu, et al. Internlm2 technical report. *arXiv preprint arXiv:2403.17297*, 2024. 1
- [4] Junsong Chen, Jincheng Yu, Chongjian Ge, Lewei Yao, Enze Xie, Yue Wu, Zhongdao Wang, James Kwok, Ping Luo, Huchuan Lu, et al. Pixart- α : Fast training of diffusion transformer for photorealistic text-to-image synthesis. *arXiv preprint arXiv:2310.00426*, 2023. 1
- [5] Keqin Chen, Zhao Zhang, Weili Zeng, Richong Zhang, Feng Zhu, and Rui Zhao. Shikra: Unleashing multimodal llm's referential dialogue magic. *arXiv preprint arXiv:2306.15195*, 2023. 3
- [6] Lin Chen, Jinsong Li, Xiaoyi Dong, Pan Zhang, Conghui He, Jiaqi Wang, Feng Zhao, and Dahua Lin. Sharegpt4v: Improving large multi-modal models with better captions. *arXiv preprint arXiv:2311.12793*, 2023. 2, 3, 5, 6, 1
- [7] Xinlei Chen, Hao Fang, Tsung-Yi Lin, Ramakrishna Vedantam, Saurabh Gupta, Piotr Dollár, and C Lawrence Zitnick. Microsoft coco captions: Data collection and evaluation server. *arXiv preprint arXiv:1504.00325*, 2015. 5, 7, 2, 3
- [8] Mehdi Cherti, Romain Beaumont, Ross Wightman, Mitchell Wortsman, Gabriel Ilharco, Cade Gordon, Christoph Schuhmann, Ludwig Schmidt, and Jenia Jitsev. Reproducible scaling laws for contrastive language-image learning. In *Proceedings of the IEEE/CVF Conference on Computer Vision and Pattern Recognition*, pages 2818–2829, 2023. 2
- [9] Wenliang Dai, Junnan Li, Dongxu Li, Anthony Meng Huat Tiong, Junqi Zhao, Weisheng Wang, Boyang Li, Pascale Fung, and Steven Hoi. Instructblip: Towards general-purpose vision-language models with instruction tuning, 2023. 3
- [10] Jia Deng, Wei Dong, Richard Socher, Li-Jia Li, Kai Li, and Li Fei-Fei. Imagenet: A large-scale hierarchical image database. In *2009 IEEE conference on computer vision and pattern recognition*, pages 248–255. Ieee, 2009. 5, 7
- [11] Xiaoyi Dong, Jianmin Bao, Yinglin Zheng, Ting Zhang, Dongdong Chen, Hao Yang, Ming Zeng, Weiming Zhang, Lu Yuan, Dong Chen, et al. Maskclip: Masked self-distillation advances contrastive language-image pretraining. In *Proceedings of the IEEE/CVF Conference on Computer Vision and Pattern Recognition*, pages 10995–11005, 2023. 2
- [12] Lijie Fan, Dilip Krishnan, Phillip Isola, Dina Katabi, and Yonglong Tian. Improving clip training with language rewrites. *Advances in Neural Information Processing Systems*, 36, 2024. 2
- [13] Roopal Garg, Andrea Burns, Burcu Karagol Ayan, Yonatan Bitton, Ceslee Montgomery, Yasumasa Onoe, Andrew Bunner, Ranjay Krishna, Jason Baldridge, and Radu Soricut. Imageinwords: Unlocking hyper-detailed image descriptions. *arXiv preprint arXiv:2405.02793*, 2024. 5, 2, 3
- [14] Xiuye Gu, Tsung-Yi Lin, Weicheng Kuo, and Yin Cui. Open-vocabulary object detection via vision and language knowledge distillation. *arXiv preprint arXiv:2104.13921*, 2021. 2
- [15] Hasan Abed Al Kader Hammoud, Hani Itani, Fabio Pizzati, Philip Torr, Adel Bibi, and Bernard Ghanem. Synthclip: Are we ready for a fully synthetic clip training? *arXiv preprint arXiv:2402.01832*, 2024. 2
- [16] Kaiming He, Haoqi Fan, Yuxin Wu, Saining Xie, and Ross Girshick. Momentum contrast for unsupervised visual representation learning. In *Proceedings of the IEEE/CVF conference on computer vision and pattern recognition*, pages 9729–9738, 2020. 5
- [17] Kaiming He, Xinlei Chen, Saining Xie, Yanghao Li, Piotr Dollár, and Ross Girshick. Masked autoencoders are scalable vision learners. In *Proceedings of the IEEE/CVF conference on computer vision and pattern recognition*, pages 16000–16009, 2022. 3
- [18] Dan Hendrycks, Kevin Zhao, Steven Basart, Jacob Steinhardt, and Dawn Song. Natural adversarial examples. In *Proceedings of the IEEE/CVF conference on computer vision and pattern recognition*, pages 15262–15271, 2021. 5, 6, 7
- [19] Jitesh Jain, Jianwei Yang, and Humphrey Shi. Vcoder: Versatile vision encoders for multimodal large language models. In *Proceedings of the IEEE/CVF Conference on Computer Vision and Pattern Recognition*, pages 27992–28002, 2024. 2
- [20] Chao Jia, Yinfei Yang, Ye Xia, Yi-Ting Chen, Zarana Parekh, Hieu Pham, Quoc Le, Yun-Hsuan Sung, Zhen Li, and Tom Duerig. Scaling up visual and vision-language representation learning with noisy text supervision. In *International conference on machine learning*, pages 4904–4916. PMLR, 2021. 2
- [21] Ranjay Krishna, Yuke Zhu, Oliver Groth, Justin Johnson, Kenji Hata, Joshua Kravitz, Stephanie Chen, Yannis Kalantidis, Li-Jia Li, David A Shamma, et al. Visual genome: Connecting language and vision using crowdsourced dense image annotations. *International journal of computer vision*, 123:32–73, 2017. 3, 1, 2
- [22] A. Krizhevsky and G. Hinton. Learning multiple layers of features from tiny images. *Handbook of Systemic Autoimmune Diseases*, 1(4), 2009. 5, 7
- [23] Zhengfeng Lai, Haotian Zhang, Bowen Zhang, Wentao Wu, Haoping Bai, Aleksei Timofeev, Xianzhi Du, Zhe Gan, Jiulong Shan, Chen-Nee Chuah, et al. Veclip: Improving clip training via visual-enriched captions. In *European Conference on Computer Vision*, pages 111–127. Springer, 2025. 2
- [24] Mengcheng Lan, Chaofeng Chen, Yiping Ke, Xinjiang Wang, Litong Feng, and Wayne Zhang. Proxyclip: Proxy attention improves clip for open-vocabulary segmentation. *arXiv preprint arXiv:2408.04883*, 2024. 1, 2
- [25] Boyi Li, Kilian Q Weinberger, Serge Belongie, Vladlen

- Koltun, and René Ranftl. Language-driven semantic segmentation. *arXiv preprint arXiv:2201.03546*, 2022. 2
- [26] Junnan Li, Dongxu Li, Caiming Xiong, and Steven Hoi. Blip: Bootstrapping language-image pre-training for unified vision-language understanding and generation. In *International conference on machine learning*, pages 12888–12900. PMLR, 2022. 1
- [27] Junnan Li, Dongxu Li, Silvio Savarese, and Steven Hoi. Blip-2: Bootstrapping language-image pre-training with frozen image encoders and large language models. In *International conference on machine learning*, pages 19730–19742. PMLR, 2023. 1
- [28] Liunian Harold Li, Pengchuan Zhang, Haotian Zhang, Jianwei Yang, Chunyuan Li, Yiwu Zhong, Lijuan Wang, Lu Yuan, Lei Zhang, Jenq-Neng Hwang, et al. Grounded language-image pre-training. In *Proceedings of the IEEE/CVF Conference on Computer Vision and Pattern Recognition*, pages 10965–10975, 2022. 2
- [29] Yanghao Li, Haoqi Fan, Ronghang Hu, Christoph Feichtenhofer, and Kaiming He. Scaling language-image pre-training via masking. In *Proceedings of the IEEE/CVF Conference on Computer Vision and Pattern Recognition*, pages 23390–23400, 2023. 2, 7
- [30] Yunheng Li, Zhongyu Li, Quansheng Zeng, Qibin Hou, and Ming-Ming Cheng. Cascade-clip: Cascaded vision-language embeddings alignment for zero-shot semantic segmentation. *arXiv preprint arXiv:2406.00670*, 2024. 1, 2
- [31] Haotian Liu, Chunyuan Li, Yuheng Li, and Yong Jae Lee. Improved baselines with visual instruction tuning. In *Proceedings of the IEEE/CVF Conference on Computer Vision and Pattern Recognition*, pages 26296–26306, 2024. 3
- [32] Haotian Liu, Chunyuan Li, Yuheng Li, Bo Li, Yuanhan Zhang, Sheng Shen, and Yong Jae Lee. Llava-next: Improved reasoning, ocr, and world knowledge, 2024. 3, 1, 2
- [33] Ilya Loshchilov and Frank Hutter. Decoupled weight decay regularization. *arXiv preprint arXiv:1711.05101*, 2017. 3
- [34] Jishnu Mukhoti, Tsung-Yu Lin, Omid Poursaeed, Rui Wang, Ashish Shah, Philip HS Torr, and Ser-Nam Lim. Open vocabulary semantic segmentation with patch aligned contrastive learning. In *Proceedings of the IEEE/CVF Conference on Computer Vision and Pattern Recognition*, pages 19413–19423, 2023. 1
- [35] Ivona Najdenkoska, Mohammad Mahdi Derakhshani, Yuki M Asano, Nanne van Noord, Marcel Worring, and Cees GM Snoek. Tulip: Token-length upgraded clip. *arXiv preprint arXiv:2410.10034*, 2024. 2, 6, 7
- [36] Vicente Ordonez, Girish Kulkarni, and Tamara Berg. Im2text: Describing images using 1 million captioned photographs. *Advances in neural information processing systems*, 24, 2011. 3, 1, 2
- [37] William Peebles and Saining Xie. Scalable diffusion models with transformers. In *Proceedings of the IEEE/CVF International Conference on Computer Vision*, pages 4195–4205, 2023. 1
- [38] Bryan A Plummer, Liwei Wang, Chris M Cervantes, Juan C Caicedo, Julia Hockenmaier, and Svetlana Lazebnik. Flickr30k entities: Collecting region-to-phrase correspondences for richer image-to-sentence models. In *Proceedings of the IEEE international conference on computer vision*, pages 2641–2649, 2015. 5, 7, 2, 3
- [39] Alec Radford, Jong Wook Kim, Chris Hallacy, Aditya Ramesh, Gabriel Goh, Sandhini Agarwal, Girish Sastry, Amanda Askell, Pamela Mishkin, Jack Clark, et al. Learning transferable visual models from natural language supervision. In *International conference on machine learning*, pages 8748–8763. PMLR, 2021. 1, 2, 6, 7, 3, 5
- [40] Benjamin Recht, Rebecca Roelofs, Ludwig Schmidt, and Vaishaal Shankar. Do imagenet classifiers generalize to imagenet? In *International conference on machine learning*, pages 5389–5400. PMLR, 2019. 5, 7
- [41] Robin Rombach, Andreas Blattmann, Dominik Lorenz, Patrick Esser, and Bjorn Ommer. High-resolution image synthesis with latent diffusion models. In *2022 IEEE/CVF Conference on Computer Vision and Pattern Recognition (CVPR)*, 2022. 1
- [42] Piyush Sharma, Nan Ding, Sebastian Goodman, and Radu Soricut. Conceptual captions: A cleaned, hypernymed, image alt-text dataset for automatic image captioning. In *Proceedings of the 56th Annual Meeting of the Association for Computational Linguistics (Volume 1: Long Papers)*, pages 2556–2565, 2018. 3, 1, 2
- [43] Bowen Shi, Peisen Zhao, Zichen Wang, Yuhang Zhang, Yaoming Wang, Jin Li, Wenrui Dai, Junni Zou, Hongkai Xiong, Qi Tian, et al. Umg-clip: A unified multi-granularity vision generalist for open-world understanding. In *European Conference on Computer Vision*, pages 259–277. Springer, 2025. 1, 2
- [44] Oriane Siméoni, Gilles Puy, Huy V Vo, Simon Roburin, Spyros Gidaris, Andrei Bursuc, Patrick Pérez, Renaud Marlet, and Jean Ponce. Localizing objects with self-supervised transformers and no labels. *arXiv preprint arXiv:2109.14279*, 2021. 2
- [45] Quan Sun, Yuxin Fang, Ledell Wu, Xinlong Wang, and Yue Cao. Eva-clip: Improved training techniques for clip at scale. *arXiv preprint arXiv:2303.15389*, 2023. 2, 7
- [46] Zeyi Sun, Ye Fang, Tong Wu, Pan Zhang, Yuhang Zang, Shu Kong, Yuanjun Xiong, Dahua Lin, and Jiaqi Wang. Alpha-clip: A clip model focusing on wherever you want. In *Proceedings of the IEEE/CVF Conference on Computer Vision and Pattern Recognition*, pages 13019–13029, 2024. 2
- [47] Bart Thomee, David A Shamma, Gerald Friedland, Benjamin Elizalde, Karl Ni, Douglas Poland, Damian Borth, and Li-Jia Li. Yfcc100m: The new data in multimedia research. *Communications of the ACM*, 59(2):64–73, 2016. 3, 1, 2
- [48] Jack Urbanek, Florian Bordes, Pietro Astolfi, Mary Williamson, Vasu Sharma, and Adriana Romero-Soriano. A picture is worth more than 77 text tokens: Evaluating clip-style models on dense captions. In *Proceedings of the IEEE/CVF Conference on Computer Vision and Pattern Recognition*, pages 26700–26709, 2024. 5, 2, 3
- [49] Jinpeng Wang, Pan Zhou, Mike Zheng Shou, and Shuicheng Yan. Position-guided text prompt for vision-language pre-training. In *Proceedings of the IEEE/CVF Conference on Computer Vision and Pattern Recognition*, pages 23242–23251, 2023. 1

- [50] Wenhui Wang, Hangbo Bao, Li Dong, Johan Bjorck, Zhiliang Peng, Qiang Liu, Kriti Aggarwal, Owais Khan Mohammed, Saksham Singhal, Subhojit Som, et al. Image as a foreign language: Beit pretraining for vision and vision-language tasks. In *Proceedings of the IEEE/CVF Conference on Computer Vision and Pattern Recognition*, pages 19175–19186, 2023. [1](#)
- [51] Wei Wu, Kecheng Zheng, Shuailei Ma, Fan Lu, Yuxin Guo, Yifei Zhang, Wei Chen, Qingpei Guo, Yujun Shen, and Zheng-Jun Zha. Lotlip: Improving language-image pre-training for long text understanding. *arXiv preprint arXiv:2410.05249*, 2024. [1](#), [2](#), [3](#), [5](#), [6](#), [7](#)
- [52] Rui Xiao, Sanghwan Kim, Mariana-Iuliana Georgescu, Zeynep Akata, and Stephan Alaniz. Flair: Vlm with fine-grained language-informed image representations. *arXiv preprint arXiv:2412.03561*, 2024. [3](#), [6](#)
- [53] Hu Xu, Saining Xie, Xiaoqing Ellen Tan, Po-Yao Huang, Russell Howes, Vasu Sharma, Shang-Wen Li, Gargi Ghosh, Luke Zettlemoyer, and Christoph Feichtenhofer. Demystifying clip data. *arXiv preprint arXiv:2309.16671*, 2023. [2](#)
- [54] Lewei Yao, Runhui Huang, Lu Hou, Guansong Lu, Minzhe Niu, Hang Xu, Xiaodan Liang, Zhenguo Li, Xin Jiang, and Chunjing Xu. Filip: Fine-grained interactive language-image pre-training. *arXiv preprint arXiv:2111.07783*, 2021. [2](#)
- [55] Qiying Yu, Quan Sun, Xiaosong Zhang, Yufeng Cui, Fan Zhang, Yue Cao, Xinlong Wang, and Jingjing Liu. Capsfusion: Rethinking image-text data at scale. In *Proceedings of the IEEE/CVF Conference on Computer Vision and Pattern Recognition*, pages 14022–14032, 2024. [2](#)
- [56] Xiaohua Zhai, Basil Mustafa, Alexander Kolesnikov, and Lucas Beyer. Sigmoid loss for language image pre-training. In *Proceedings of the IEEE/CVF international conference on computer vision*, pages 11975–11986, 2023. [6](#)
- [57] Beichen Zhang, Pan Zhang, Xiaoyi Dong, Yuhang Zang, and Jiaqi Wang. Long-clip: Unlocking the long-text capability of clip. *arXiv preprint arXiv:2403.15378*, 2024. [1](#), [2](#), [3](#), [5](#), [6](#), [7](#), [8](#), [4](#)
- [58] Jingyi Zhang, Jiaxing Huang, Sheng Jin, and Shijian Lu. Vision-language models for vision tasks: A survey. *IEEE Transactions on Pattern Analysis and Machine Intelligence*, 2024. [2](#)
- [59] Yi Zhang, Meng-Hao Guo, Miao Wang, and Shi-Min Hu. Exploring regional clues in clip for zero-shot semantic segmentation. In *Proceedings of the IEEE/CVF Conference on Computer Vision and Pattern Recognition*, pages 3270–3280, 2024. [2](#)
- [60] Kecheng Zheng, Yifei Zhang, Wei Wu, Fan Lu, Shuailei Ma, Xin Jin, Wei Chen, and Yujun Shen. Dreamlip: Language-image pre-training with long captions. In *European Conference on Computer Vision*, pages 73–90. Springer, 2025. [1](#), [2](#), [3](#), [7](#)
- [61] Ziqin Zhou, Yinjie Lei, Bowen Zhang, Lingqiao Liu, and Yifan Liu. Zegclip: Towards adapting clip for zero-shot semantic segmentation. In *Proceedings of the IEEE/CVF Conference on Computer Vision and Pattern Recognition*, pages 11175–11185, 2023. [2](#)

FIX-CLIP: Dual-Branch Hierarchical Contrastive Learning via Synthetic Captions for Better Understanding of Long Text

Supplementary Material

6. Prompting Templates for Long-text Caption Synthesis

To ensure the diversity of the synthesis long-text captions, we have set up multiple prompts to instruct Llama3-LLaVA-NeXT-8b [32] to generate long-text captions with detailed descriptions. During the re-caption process, samples are randomly taken from the following 20 prompts.

1. Provide a comprehensive description of this image, including all visual elements, their spatial relationships, and the overall atmosphere.
2. Generate a detailed caption explaining what's happening in this image, covering actions, subjects, environment, and temporal context.
3. Analyze this image in detail, describing the main subjects, background, lighting, colors, and composition.
4. Write an extensive caption that captures both the explicit visual content and implicit context or story behind this image.
5. Describe this image as if explaining it to someone who cannot see it, including all relevant details and visual nuances.
6. Break down the scene components in this image, detailing the foreground, middle ground, and background elements.
7. Describe the environmental context, lighting conditions, time of day, and weather elements visible in this image.
8. Analyze the spatial arrangement and relationships between all objects and subjects in this image.
9. Detail the setting of this scene, including architectural elements, natural features, and atmospheric conditions.
10. Explain the visual dynamics of this scene, including movement, direction, and flow of elements.
11. Elaborate on the image's details such as the objects' textures, the direction of shadows, and how they contribute to the overall look.
12. Describe the image from top to bottom and left to right, highlighting every

element and its significance within the frame.

13. Generate a caption that delves into the emotional undertones suggested by the image's colors, expressions of the subjects, and the setting.
14. Analyze the image to explain how the placement of elements affects the flow and balance within the visual space.
15. Write a detailed description of the image that includes the sizes of the objects relative to each other and their proximity.
16. Describe the image in terms of the contrast between light and dark areas and how it shapes the perception of the scene.
17. Generate a caption that interprets the possible narrative connections between different elements in the image.
18. Analyze the image to explain how the colors interact with each other and what mood they create together.
19. Write a detailed description of the image that covers the small details often overlooked, like tiny patterns on objects.
20. Describe the image by focusing on the perspective used and how it makes the viewer experience the scene.

7. Abnormal Synthesized Captions

While synthesized captions provide detailed descriptions, MLLMs usually bring hallucination elements. We apply a simple filtering method on captions to reduce repeated words, meaningless sentences, and short results. Fig. 6 shows some abnormal synthesized captions that have been cleaned out from our training datasets.

8. Details of the Setup

8.1. Details of the training datasets

Our model's training corpus comprises six distinct datasets, as enumerated in Tab. 8. The ShareGPT4V [6] dataset, previously employed in Long-CLIP [57] implementation, exhibits exceptional annotation quality. The remaining five established datasets, including CC3M [42], VisualGenome [21], SBU [36], CC12M [42], and YFCC15M [47], underwent

	Model	DCI		IIW		ShareGPT4V-1k		Urban-1k		Avg.
		I-to-T	T-to-I	I-to-T	T-to-I	I-to-T	T-to-I	I-to-T	T-to-I	
B/16	Raw Short Caption	66.2	67.1	97.1	96.7	97.8	97.6	87.7	90.1	87.5
	Synthesis Short Caption	67.1	67.5	96.9	96.7	98.1	97.9	88.0	90.8	87.9
L/14	Raw Short Caption	66.5	69.1	97.3	97.0	97.4	97.6	87.9	92.6	88.1
	Synthesis Short Caption	68.1	69.9	97.1	97.2	98.5	98.0	88.1	93.0	88.7

Table 10. Train on 5M synthesis long captions as the long-text input, we compare the performance between the raw short captions and the synthesis short captions as the short-text input. The R@1 of long-text-image retrieval on DCI [48], IIW [13], ShareGPT4V-1k [6], and Urban-1k [57] datasets. The best results are in **bold**.

	Model	COCO						Flickr30k						Avg. R@1
		Image-to-Text			Text-to-Image			Image-to-Text			Text-to-Image			
		R@1	R@5	R@10	R@1	R@5	R@10	R@1	R@5	R@10	R@1	R@5	R@10	
B/16	Raw Short Caption	61.0	84.5	90.8	44.6	70.4	79.5	89.2	98.4	99.7	77.4	94.6	97.2	68.0
	Synthesis Short Caption	61.3	84.9	91.2	47.0	72.4	81.4	89.9	98.8	99.7	78.4	95.2	97.7	69.2
L/14	Raw Short Caption	62.5	85.6	91.4	48.5	73.6	82.1	92.3	99.3	99.7	81.7	95.9	97.9	71.2
	Synthesis Short Caption	63.2	85.8	91.5	50.5	75.4	83.6	92.5	99.1	99.9	82.5	96.6	98.2	72.1

Table 11. Train on 5M synthesis long captions as the long-text input, we compare the performance between the raw short captions and the synthesis short captions as the short-text input. Results of short-caption text-image retrieval on the 5k COCO2017 [7] validation set and the 1k Flickr30K [38] test set. The best results are in **bold**.

divergence between the original text encoder and our text encoder, the model is restrained to generate coarse images. Therefore, an image-to-image refiner model is utilized subsequently to transfer the coarse images to fine images. The final performance is illustrated in Fig. 8. The result of Long-CLIP [57] has confusion in some details, *i.e.* the background, the direction, and the position relation. Even hallucinations would occur, such as the airplane equipping four jet engines in the 4-th case. For the comparison, our model correctly describes the detailed information and performs better.

10. Raw Short Caption versus Synthesis Short Caption

We identified quality limitations in the raw short captions within our training dataset through empirical observation. To address this constraint, we proposed an alternative approach utilizing synthetically generated short captions as model inputs. We conducted comprehensive comparative analyses between models trained on synthetic short captions versus those trained on raw short captions, with results presented in Tab. 10 and Tab. 11. The synthetic short captions were generated by Shikra [5]. Quantitative evaluations demonstrate that incorporating synthetic short captions into the training dataset yields substantial performance gains, suggesting the effectiveness of our proposed approach.

11. Visualization of the Similarity Heatmap

We visualize the heatmap of similarity between image features and text features, and compare our results with those of CLIP [39] and Long-CLIP [57], as shown in Fig. 9. To evaluate the performance on short texts, the prompt is set as

Configuration	FIX-CLIP Training
Batch size	2048
Training Epoch	6
Learning Rate	1e-6
Warm-up Steps	200
LR Scheduler	cosine
Optimizer	AdamW [33]
Optimizer hyper-parameters	$\beta_1, \beta_2, \epsilon = 0.9, 0.999, 1e-8$
Weight decay	1e-2

Table 12. Summary of FIX-CLIP training hyperparameters.

	COCO		Urban1k		DCI	
	I2T	T2I	I2T	T2I	I2T	T2I
Default	62.0	46.7	87.0	86.8	65.1	66.7
Shared Prompts	60.7	46.0	85.2	86.1	62.9	65.5
R2P	60.3	46.0	85.8	85.7	63.1	65.3
P2R	61.5	46.3	86.6	86.1	64.3	66.1
Short PE (len=77)	61.2	46.3	77.8	75.4	56.3	59.1
Long PE (len=248)	62.0	46.7	87.0	86.8	65.1	66.7

Table 13. Above: ablations on the efficacy of region prompts and masks. “Shared Prompts” refers to all the layers utilizing the same shared prompts, “R2P” and “P2R” denote regional prompts attending to all patch embeddings and vice versa. Bottom: the performance comparison of different position embeddings.

”a photo of $[CLS]$ ”. FIX-CLIP demonstrates superior performance over CLIP [39], accurately identifying instances in the image, as illustrated in Fig. 9a. For long-text understanding, the prompt consists of a major sentence split from the original long-text captions, enabling a direct comparison with Long-CLIP [57]. The corresponding performance is depicted in Fig. 9b.

Descriptions

This is a photo of a stone fountain with statues around it with a large building on its left and a large, more ornate building on its right. The stone fountain has a crafted base with a symbol in its middle and has black benches surrounding it. There are people standing and walking around in the background between the buildings. Smaller sections of a building can be seen on either end. The sky has a lot of thin clouds and *there's a mountain or hill range in the background*. There are also little building roof coverings on each side, perhaps for the people to take shade in or sit under. There are multiple street lights behind the stone fountain as well.

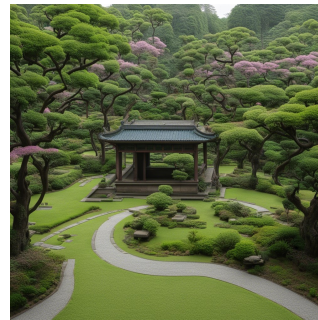
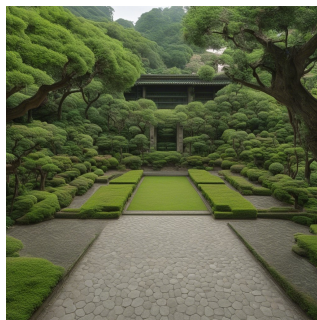
LongCLIP



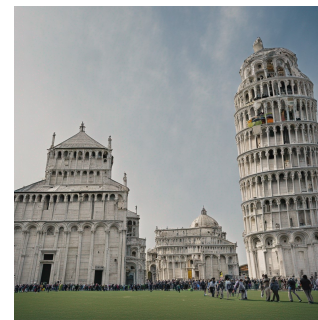
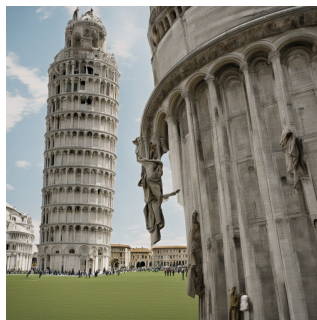
Fix-CLIP (Ours)



A garden is shown in the photo. A pinkish pathway extends from the lower left side of the image to just right of the image center. Along this pathway, thin, slab-like carved stones are staggered along both sides. *A small, green shrub is planted behind them in the lower right corner of the image*. At the end of the pathway, an open-air structure consists of a slightly raised ground slab, four blue cylindrical supports and a roof built in a traditional architectural style. Behind this structure, tall, leafy green trees are partially visible. The sky that peeks through the branches is bright white.



The Pisa Cathedral with the Leaning Tower of Pisa behind it is the focus of an eye-level, long shot on a clear day with many tourists near the Italian landmark. The front and right side of the cathedral face the viewer as it is positioned angled toward the left. The cathedral is off-white with some weathered yellow along the bottom side. The three tall front doors are open, and people mill about in the distance in front of the entrance. *The dome rises behind the cathedral. The Leaning Tower is behind the church to the right*. In the front and side of the cathedral is an expansive empty green lawn.



A Lufthansa airplane taxis to the right on a light-grey airstrip under a light-grey sky in a full outdoor shot. The airplane is white on the top three-quarters and grey on the bottom one-quarter. *It has two jet engines, one on either side, plus a blue tail with a yellow circular symbol*. The word "Lufthansa" is printed on the side of the airplane in dark-blue. The field in front of the airstrip has short green grass and short brown grass. The far side of the airstrip is mostly short brown grass, behind which are low off-white-and-grey buildings.

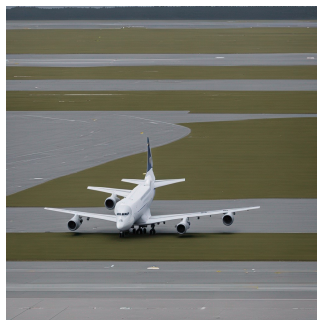
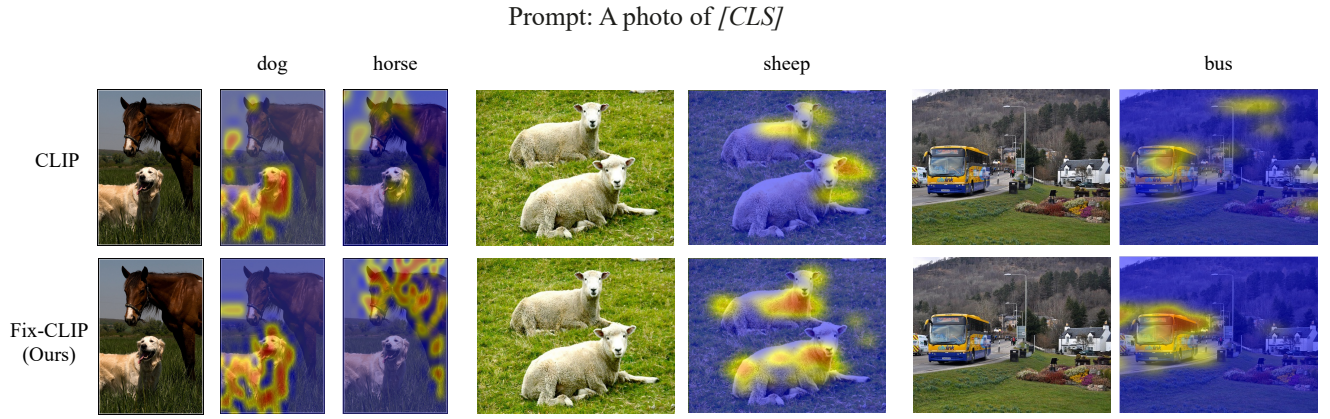
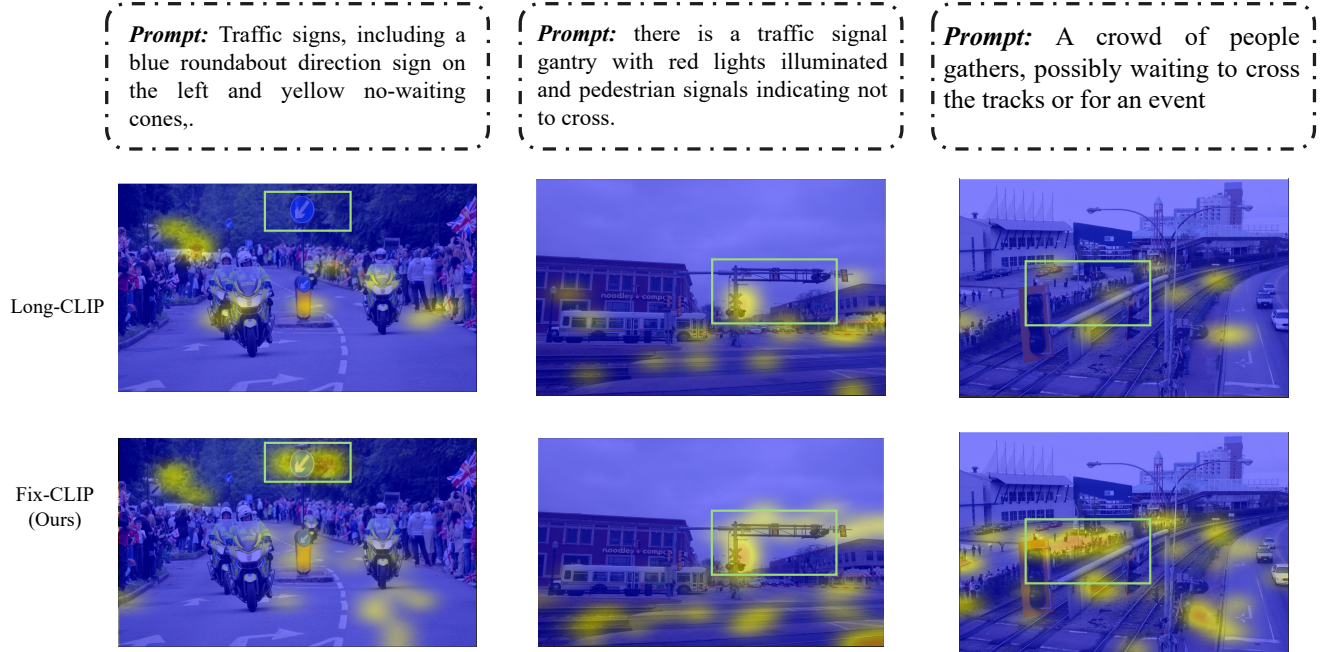


Figure 8. More Text-to-Image Generation examples. Images generated by FIX-CLIP are more accurate in detail information such as color, direction, position, quantity, material, light, and shooting angle. The text highlighted in green represents fine-grained details that Long-CLIP [57] fails to capture, whereas our proposed model FIX-CLIP successfully generates these contextual elements with high fidelity.



(a) Similarity heatmap compared with CLIP [39].



(b) Similarity heatmap compared with Long-CLIP [57].

Figure 9. Similarity Heatmap between text and image features in different models. (a) presents a comparative analysis between our model and CLIP [39] in short-text scenarios, while (b) illustrates the performance comparison between our model and Long-CLIP [57] in long-text contexts. The text segments highlighted in red represent semantic information successfully comprehended by our model but not accurately captured by Long-CLIP [57].